The Journal of Neuroscience, August 1993, 13(8): 3211–3221

Calcium Current Block by (−)-Pentobarbital, Phenobarbital, and CHEB but not (+)-Pentobarbital in Acutely Isolated Hippocampal CA1 Neurons: Comparison with Effects on GABA-activated Cl^- Current

Jarlath M. H. ffrench-Mullen,[1] Jeffery L. Barker,[2] and Michael A. Rogawski[3]

[1]Department of Pharmacology, Zeneca Pharmaceuticals Group, Zeneca Inc., Wilmington, Delaware 19897 and [2]Laboratory of Neurophysiology, and [3]Neuronal Excitability Section, Epilepsy Research Branch, National Institute of Neurological Disorders and Stroke, National Institutes of Health, Bethesda, Maryland 20892

Block of a voltage-activated Ca^{2+} channel current by phenobarbital (PHB), 5-(2-cyclohexylideneethyl)-5-ethyl barbituric acid (CHEB), and the optical *R*(−)- and *S*(+)-enantiomers of pentobarbital (PB) was examined in freshly dissociated adult guinea pig hippocampal CA1 neurons; the effects of the barbiturates on GABA-activated Cl^- current were also characterized in the same preparation. (−)-PB, PHB, and CHEB produced a reversible, concentration-dependent block of the peak Ca^{2+} channel current (3 mM Ba^{2+} as the charge carrier) evoked by depolarization from −80 to −10 mV (IC_{50} values, 3.5, 72, and 118 μM, respectively). In contrast, (+)-PB was nearly inactive at concentrations up to 1 mM. The inhibitory action of PHB was decreased at acid pH, indicating that the dissociated (anionic) form of the molecule is the active species. Block by (−)-PB was voltage dependent with the fractional block increasing at positive membrane potentials; calculations according to the method of Woodhull indicated that the (−)-PB blocking site senses ~40% of the transmembrane electric field. The time course and voltage dependence of activation of the Ca^{2+} channel current were unaffected by (−)-PB, PHB, and CHEB. The rate of inactivation was enhanced by (−)-PB and CHEB, with the major effect being acceleration of the slow phase of the biexponential decay of the current. GABA-activated Cl^- current was potently enhanced by (−)-PB and PHB (EC_{50} values, 3.4 and 12 μM), whereas (+)-PB was only weakly active. At concentrations of (−)-PB > 100 μM and PHB > 200–300 μM, Cl^- current responses were activated even in the absence of GABA. These results demonstrate that in CA1 hippocampal neurons, PB causes a stereoselective block of a voltage-activated Ca^{2+} current; PHB is also effective, but at higher concentrations. For (−)-PB, the effect on Ca^{2+} channel current occurred at similar concentrations as potentiation of GABA responses. In contrast, PHB was more potent as a GABA enhancer than as blocker of Ca^{2+} current, but the maximal potentiation of GABA responses was 40% of that obtained with (−)-PB. Consequently, the anticonvulsant action of PHB at clinically relevant concentrations may relate to modest enhancement of GABA responses and partial blockade of Ca^{2+} current, whereas the sedative effects that occur at higher concentrations could reflect stronger Ca^{2+} current blockade. The powerful sedative–hypnotic action of (−)-PB may reflect greater maximal enhancement of GABA responses in conjunction with strong inhibition of Ca^{2+} current. The convulsant action of CHEB is unlikely to be related to its effects on the Ca^{2+} current.

[Key words: calcium channel, GABA receptor, (−)-pentobarbital, (+)-pentobarbital, phenobarbital, CHEB [5-(2-cyclohexylideneethyl)-5-ethyl barbituric acid], CA1 hippocampal neuron, voltage-clamp recording]

Barbiturates are used clinically for their sedative, hypnotic, general anesthetic, and anticonvulsant actions (Rall, 1990). However, there are important differences among the pharmacological properties of structurally similar barbiturates. For example, phenobarbital (PHB) is an anticonvulsant that produces minimal sedation at clinically effective doses, whereas pentobarbital (PB) is a powerful CNS depressant at anticonvulsant doses and is therefore unsuitable for use in epilepsy therapy (Rogawski and Porter, 1990). Moreover, certain barbiturate analogs, such as 5-(2-cyclohexylideneethyl)-5-ethyl barbituric acid (CHEB), have convulsant activity (Andrews et al., 1982). These pharmacological differences have been attributed to differences in the profile of action of the various barbiturate analogs on neurotransmitter- and voltage-gated ion channel systems in CNS neurons. Among the best recognized cellular actions of barbiturates is enhancement of GABA-activated Cl^- conductance, which occurs at low micromolar concentrations (Olsen, 1988; Macdonald et al., 1989), and GABA-independent activation of the $GABA_A$ receptor channel, which occurs at higher but still clinically relevant concentrations (Mathers and Barker, 1980; Parker et al., 1986). Structure–activity studies are consistent with the view that the sedative and anesthetic effects of barbiturates are mediated via their interaction with $GABA_A$ receptors (Olsen, 1988). However, the GABA hypothesis does not explain differences in the activity profiles of the various barbiturate analogs. These differences could be due to actions of the drugs on other target sites. In this regard, blockade of voltage-activated Ca^{2+} channels, particularly those in nerve terminals that mediate excitatory synaptic neurotransmitter release, is a particularly attractive non-GABA mechanism. In fact, barbiturates are well known to inhibit neurotransmitter release (Brooks and Eccles, 1947; Weakly, 1969; Richards, 1972) and have been demonstrated to block Ca^{2+} entry into presynaptic nerve ter-

Nov. 20, 1992; revised Feb. 10, 1993; accepted Feb. 16, 1993.

Correspondence should be addressed to Jarlath M. H. ffrench-Mullen, Ph.D., Department of Pharmacology, Zeneca Pharmaceuticals Group, Zeneca Inc., Wilmington, DE 19897-2500.

minals (Blaustein and Ector, 1975; Morgan and Bryant, 1977; Leslie et al., 1980). N-type and also L-type Ca^{2+} channels may provide the pathway for the Ca^{2+} entry that triggers transmitter release (Miller, 1990; Stanley, 1991). In voltage-clamp studies carried out with vertebrate (Werz and Macdonald, 1985) and invertebrate (Nishi and Oyamura, 1983; Ikemoto et al., 1986) neurons, PB and PHB were found to block Ca^{2+} current, with a selectivity for N- and L-type Ca^{2+} channels (Gross and Macdonald, 1988). A reduction of an N-type Ca^{2+} current by PB and PHB was also observed in *Xenopus* oocytes injected with human brain mRNA (Gundersen et al., 1988). In all of these studies, high (supratherapeutic) concentrations were required (typically 0.1–1 mM for PB) and no compelling structure–activity data were presented for a correlation between Ca^{2+} current blocking potency and CNS depressant activity, so the role of Ca^{2+} channel blockade in the various pharmacological actions of barbiturates has remained uncertain (Olsen, 1988). Demonstration of a stereoselective action would be of particular significance since, for barbiturates like PB that have a chiral center, the *S*(−) isomers are well known to have greater CNS depressant activity than the *R*(+) isomers (Waddell and Baggett, 1973). Recently, it has become apparent that there is great diversity among neuronal Ca^{2+} channels with respect to their sensitivity to pharmacological blockade (Bean, 1989; Regan et al., 1991; Mintz et al., 1992). Therefore, in the present study we compared the activity of several barbiturates, including the optical enantiomers of PB, on Ca^{2+} channel and GABA-activated Cl^- currents in acutely isolated guinea pig hippocampal neurons. Our data support the concept that differences in the profile of activity at Ca^{2+} channels and GABA-activated Cl^- channels may account for the distinctive properties of the pharmacologically dissimilar barbiturates.

Materials and Methods

Cell preparation. Pyramidal neurons were acutely isolated form the CA1 region of the mature guinea pig hippocampus according to methods described by Kay and Wong (1986). In brief, 1 mm^3 tissue chunks were dissected by hand from the hippocampus of 200–300 gm guinea pigs. The chunks were digested at 37°C for 40–50 min under a pure oxygen atmosphere in PIPES [piperazine-*N*,*N*′-bis(2-ethanesulfonic acid)]-buffered saline of the following composition (in mM, except as noted): NaCl, 120; KCl, 5; $CaCl_2$, 1; $MgCl_2$, 1; D-glucose, 25; PIPES, 20; and trypsin (type XI; Sigma Chemical Co., St. Louis, MO), 0.5 mg/ml (pH, 7.0). The trypsin-containing PIPES/saline was then replaced with enzyme-free solution and left at room temperature for <2 hr. Cells were isolated as needed by trituration of six tissue chunks in 1 ml of 20 mM HEPES-buffered Dulbecco's modified Eagle's medium (DMEM). The cell suspension was plated onto a 35 mm polystyrene petri dish, and the cells were allowed to settle for 7–10 min before the DMEM was aspirated and replaced with recording medium.

Whole-cell recording. Macroscopic whole-cell Ca^{2+} channel currents were recorded at room temperature (19–25°C) using 3 mM Ba^{2+} as the external charge-carrying divalent cation, and with the Ca^{2+} chelator Cs_4-BAPTA (Molecular Probes, Eugene, OR) in the intracellular solution to reduce Ca^{2+}-promoted Ca^{2+} channel inactivation (Eckert and Chad, 1984). The bath solution contained (in mM) $BaCl_2$, 3; tetraethylammonium chloride (TEA-Cl), 140; $MgCl_2$, 1; HEPES, 10; glucose, 6; and TTX, 0.002. The solution was adjusted to a pH of 7.4 with fresh CsOH solution and to an osmolality of 320 mOsm/kg H_2O. The pipette solution contained (in mM) *N*-methyl-D-glucamine chloride, 120; Cs_4-BAPTA, 5; and Mg-ATP, 5. The ATP regeneration system Tris-phosphocreatinine (20 mM) and creatine kinase (20 U/ml) was added to the internal solution to minimize rundown of the Ca^{2+} currents (Forscher and Oxford, 1985; Byerly and Yazejian, 1986). The internal solution was adjusted to pH 7.2 with fresh CsOH and to an osmolality of 315 mOsm/kg H_2O. The rate of rundown under these conditions was <5% over a 30 min period (verified in five control cells). GABA-activated currents were recorded with the same internal pipette solution as Ca^{2+} channel currents and with the following bath solution (in mM): NaCl, 120; CsCl, 5; $CaCl_2$, 2; $MgCl_2$, 1; TEA-Cl, 15; 4-aminopyridine, 5; HEPES, 10; and glucose, 25. The solution was adjusted to a pH of 7.4 and an osmolality of 320 mOsm/kg H_2O.

Recordings were carried out using the whole-cell patch-clamp technique. Patch electrodes were prepared from 1.5 mm o.d. filament fused, borosilicate glass capillaries (Kwik-Fil TW 150F, WPI Instruments, New Haven, CT) using a Sutter-Brown P-87 horizontal puller (Sutter Instruments, CA). Pipette-to-bath resistances prior to seal formation were typically 3–7 MΩ; seal resistances were >10 GΩ. Liquid junction potentials between the electrode solution and the bath were minimized by placement of the reference electrode in a compartment filled with the pipette solution that was electrically connected to the recording chamber by an agar bridge. Whole-cell currents were recorded with an Axopatch 1D patch-clamp amplifier (Axon Instruments, Foster City, CA). Following seal formation and prior to entering the whole-cell mode, electrode capacitance was neutralized by using the capacitance compensation circuitry of the Axopatch. In the whole-cell mode, the Axopatch was further adjusted to correct for 80–85% of the series resistance (2–4 MΩ).

Command potential sequences were delivered to the patch-clamp amplifier and data was simultaneously acquired under computer control. Evoked currents were filtered at 10 kHz (−3 dB, eight-pole low-pass Bessel filter; Frequency Devices, Haverhill, MA), digitally sampled at 500 μsec per point (50 μsec per point for tail current measurements), and stored on magnetic media in digital form for later analysis. Capacitative and leakage currents were digitally subtracted from all records on line with the PCLAMP 5.51 (Axon Instruments) software package. Capacitative transients decayed with a time constant of 100 μsec.

Drug application. A rapid superfusion system consisting of a side-by-side array of six 200 μm i.d. (100 μm for the GABA solutions) capillary tubes was positioned within 400 μM of the cell under study. Drug solutions were applied by gravity feed and flow was computer controlled via solenoid valves. Solution changes were accomplished within 200–500 msec. GABA was applied at 1–3 min intervals to prevent desensitization. The recording chamber was continuously perfused at all times during the experiment with drug-free solution at a flow rate of 1.5 ml/min.

Data analysis. Percentage block was determined according to the formula $100 \times (1 - I_{drug}/I_{control})$, where $I_{control}$ is the leak-subtracted peak current amplitude prior to the drug application and I_{drug} is the peak current amplitude in the presence of the test drug. All traces are the average of three steps and are leak subtracted. During the drug applications, the Ca^{2+} current was repetitively evoked at intervals of 15, 30, and 180 sec for the 10, 200, and 1000 msec duration depolarizing step protocols, respectively. When exposed to the barbiturates, the peak current gradually diminished during the 20–90 sec period after the onset of the drug superfusion. An additional 60 sec was allowed to elapse upon achieving this steady-state level before the measurement of drug block was made. The slow onset of block presumably results from restricted access of the barbiturates to their blocking site; there was no evidence of use-dependent block (see Results). Concentration–effect data were fit with a nonlinear least-squares program (NFIT, Island Products, Galveston, TX) according to the logistical equation

$$B = \frac{100}{1 + (IC_{50}/[DRUG])^{n_H}}, \quad (1)$$

where [DRUG] is the drug concentration, IC_{50} is the concentration resulting in 50% block, and n_H is an empirical parameter that describes the steepness of the curve and has the same meaning as the Hill coefficient. Decay rates were fit to either single or double exponential functions using NFIT. Tail current amplitudes were estimated by fitting the falling phase of the current to a single exponential function and extrapolating the curve to zero time. Concentration–response data for barbiturate potentiation of GABA currents were fit to the equation

$$P = \frac{P_{max}}{1 + (EC_{50}/[DRUG])^{n_H}}, \quad (2)$$

where P is the percentage potentiation, P_{max} is the maximal percentage potentiation, and EC_{50} is the concentration resulting in 50% maximal

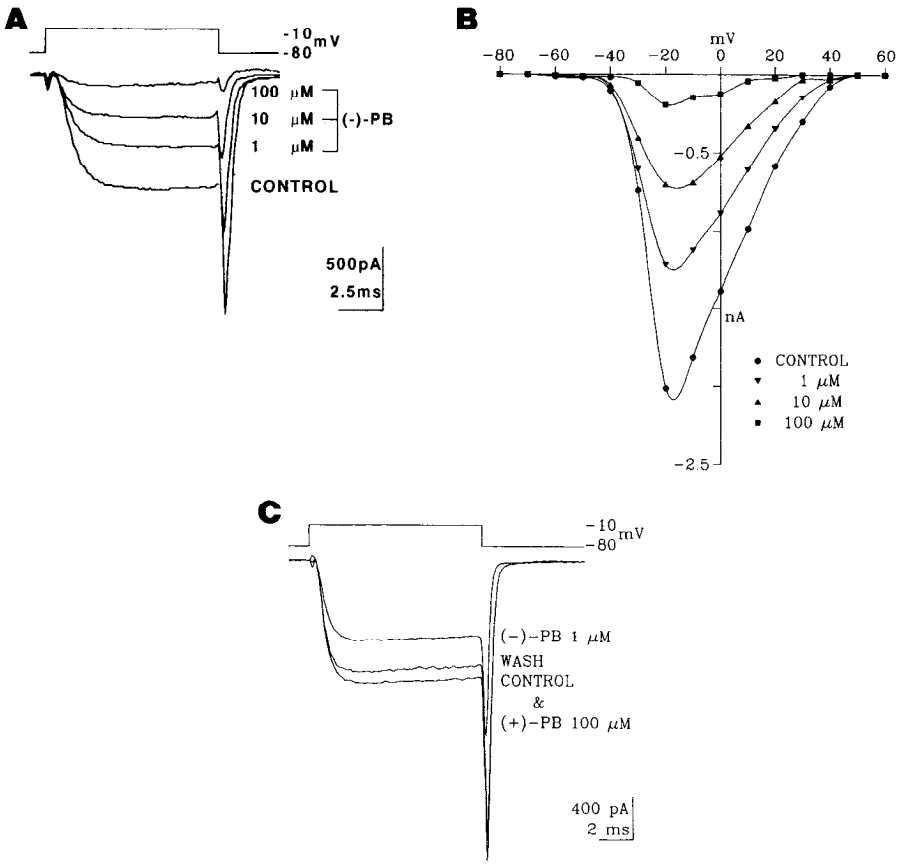

Figure 1. PB blocks I_{Ca} in a concentration-dependent and stereospecific manner. Currents were evoked in guinea pig CA1 hippocampal neurons using Ba^{2+} as the charge carrier. *A*, Increasing concentrations of (−)-PB produced a progressive depression of I_{Ca} and the corresponding tail currents. *B*, Current–voltage plot for the experiment illustrated in *A* (current amplitude measured 0.5 msec prior to the end of the 10 msec step) under control conditions and after exposure to increasing concentrations of (−)-PB; the data points are connected by cubic splines. *C*, In another neuron, perfusion with 100 μM (+)-PB has no effect on the amplitude of the current evoked with voltage steps from −80 to −10 mV. Inclusion of 1 μM (−)-PB in the (+)-PB–containing solution depresses I_{Ca} and its corresponding tail current; partial recovery is obtained upon wash with (+)-PB solution.

potentiation. All quantitative data are expressed as the mean ± SEM; *n* indicates the number of cells examined.

Materials. (+)- and (−)-pentobarbital, phenobarbital, and CHEB were obtained from the Research Triangle Institute, Research Triangle Park, NC. All other chemicals were obtained from Sigma.

Results

The data presented in this report represent the results of whole-cell recordings from 113 acutely dissociated adult guinea pig hippocampal CA1 neurons.

I_{Ca} *in acutely dissociated guinea pig hippocampal CA1 neurons*

Macroscopic voltage-gated whole-cell Ca^{2+} channel currents (I_{Ca}) were recorded using 3 mM Ba^{2+} as the charge-carrying cation. Depolarizing voltage steps from −80 mV to various potentials positive to −60 mV elicited a high-threshold inward current that peaked rapidly and decayed gradually with maintained depolarization (see, e.g., Figs. 1, 2, 8). Superfusion with 50 μM Cd^{2+} virtually eliminated (98 ± 1% block; $n = 4$) the inward current (Fig. 2*A*), demonstrating that it is carried by Ca^{2+} channels. The absence of any detectable voltage-dependent outward current in the leak-subtracted recordings after exposure to Cd^{2+} indicated that K^+ currents were effectively eliminated under the recording conditions we used. The current–voltage relationship of the macroscopic Ca^{2+} channel current was smooth and peaked at −20 mV (Fig. 1*B*).

In the subsequent pharmacological studies, we determined the current amplitude at its peak so as to maximize the contribution of the inactivating (N-type) Ca^{2+} channel currents. At times other than the peak of the Ca^{2+} current, we used tail currents to quantitate the Ca^{2+} conductance. Tail currents recorded at −80 mV were generally well fit by a single exponential function; the time constant of decay of the tail current at −80 mV in drug-free solution was generally ~200–300 msec. We did not attempt to determine the relative contribution of N, P-, or other Ca^{2+} channel types to the high-threshold current (Regan et al., 1991; Mintz et al., 1992); T-type channels are not present in CA1 neurons (Thompson and Wong, 1991).

PB stereoselectively depresses I_{Ca}

The effects of (−)-PB were concentration dependent (Fig. 1*A*) and reversible at low concentrations. At concentrations of 10 μM or less, 80–100% recovery was consistently seen within 5 min of switching to the wash solution. With concentrations ≥100 μM, there was 60–80% recovery within the same time period. As illustrated by the family of current–voltage curves in Figure 1*B*, (−)-PB produced a concentration-dependent depression of I_{Ca} at all voltages without altering the shape of the current–voltage relationship. As illustrated in Figure 1*C*, 100 μM (+)-PB had minimal effect on I_{Ca}. However, changing to a solution containing 1 μM (−)-PB in addition to the (+)-PB caused a suppression of I_{Ca} that partially reversed upon returning to the solution containing (+)-PB alone. We evaluated the possible use-dependence of the block in experiments where I_{Ca} was repetitively activated with 5–10-msec-duration voltage steps at stimulus intervals of 1, 5, 10, and 30 sec applied after an equilibration period of 2 min. In three cells evaluated in this manner, we failed to observe a progressive development of block during the stimulus train.

In contrast to the effects of (−)-PB, 100 μM (+)-PB caused very little depression of I_{Ca} (2.9 ± 1.2% block; $n = 6$; Fig. 1*C*). At 1 mM, the highest concentration examined, there was still only a modest block (18 ± 2%; $n = 3$).

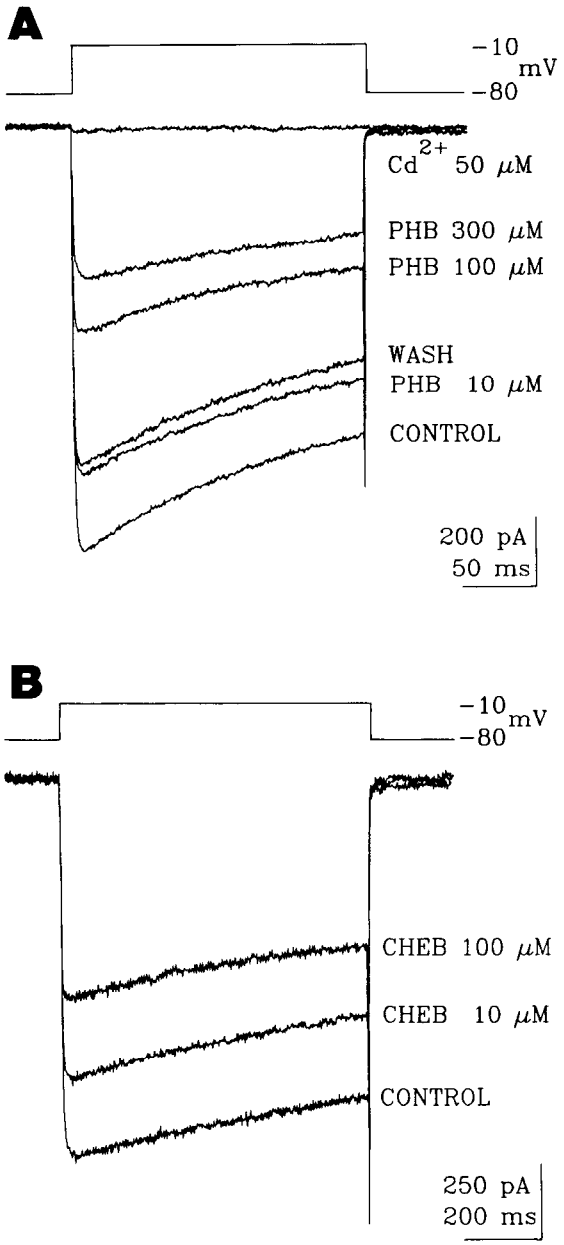

Figure 2. Concentration-dependent block of I_{Ca} by PHB and CHEB in two different cells. In *A*, the wash record was obtained after exposure to the highest drug concentration; following wash the current was virtually completely blocked by perfusion with 50 μM Cd^{2+}.

PHB and CHEB also depress I_{Ca} but are less potent than (−)-PB

The anticonvulsant barbiturate PHB also reversibly depressed I_{Ca} in a concentration-dependent manner (Fig. 2*A*). For the cell shown in Figure 2*A*, the peak current was depressed to 35% of the control value by 300 μM PHB, but recovered to 80% of the control value during subsequent perfusion with control solution (4 min). Like (−)-PB and PHB, the convulsant barbiturate CHEB also depressed I_{Ca} in a concentration-dependent manner (Fig. 2*B*). Both PHB and CHEB failed to alter the shape of the current–voltage relationship for the peak current (three cells studied with each drug; data not shown). As was the case with (−)-PB, PHB failed to exhibit a use-dependent blocking action in experiments with stimulus trains (n = 2).

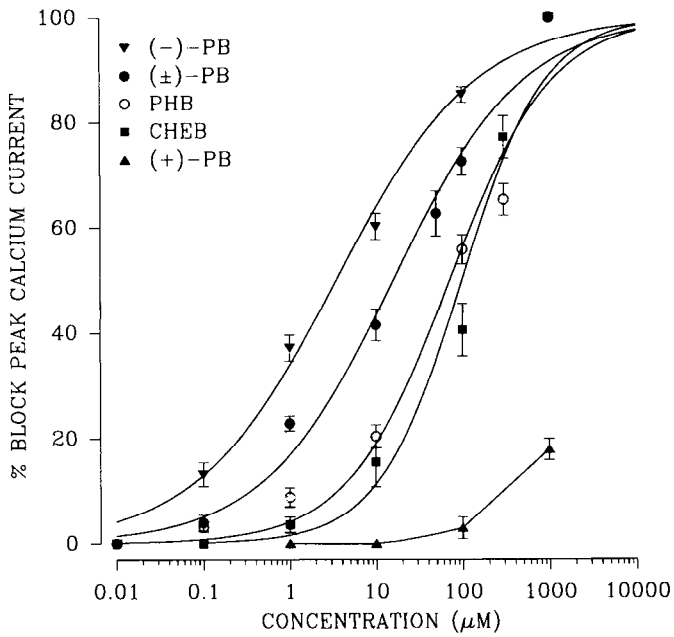

Figure 3. Concentration–response curves for depression of peak I_{Ca} by (−)-, (+)-, and (±)-PB, PHB, and CHEB. Each point represents the mean ± SEM of data from three to eight cells.

The concentration–effect relationships for inhibition of the peak Ca^{2+} current by (−)- and (+)-PB, (±)-PB, PHB, and CHEB are shown in Figure 3. The IC_{50} values were 3.5, 72, and 118 μM and the Hill coefficients (n_H) were 0.5, 0.7, and 1 for (−)-PB, PHB, and CHEB, respectively (Table 1); (+)-PB failed to cause 50% block even at concentrations as high as 1 mM. The IC_{50} for (±)-PB was 16 μM, a value intermediate to that of the optical isomers (n_H, 0.7). All of the compounds, with the exception of (+)-PB, produced total block of the Ca^{2+} current at 1 mM.

The activity of PHB decreases at acid pH

Among therapeutically useful barbiturates (barbituric acid derivatives), PHB is unusually acidic. Because its pK_a value (7.29; Vida and Gerry, 1977) is close to the physiological pH (7.40), PHB is normally present in both the undissociated (44%) and dissociated (56%) forms and small shifts in the pH of the external medium will result in large changes in the extent to which the drug is ionized. We examined whether the effect of PHB on I_{Ca} was attributable to the anion or the free acid by applying the drug in solutions of different acidic pH values. Figure 4 indicates the percentage block obtained with 10 μM PHB in solutions with pH values of 6.50–7.40. The titration curve for the acidic car-

Table 1. IC_{50} values for blockade of I_{Ca} and EC_{50} values for potentiation of GABA-activated Cl^- currents in isolated CA1 neurons

Barbiturate	$I_{Ca}IC_{50}$ (μM)	GABA EC_{50} (μM)	GABA P_{max} (%)
(−)-PB	3.5	3.4	1366
(+)-PB	>1000	>1000	
PHB	72	12	600
CHEB	118	ND	ND

I_{Ca} IC_{50} values were determined from Equation 1; GABA EC_{50} and P_{max} values were from Equation 2.

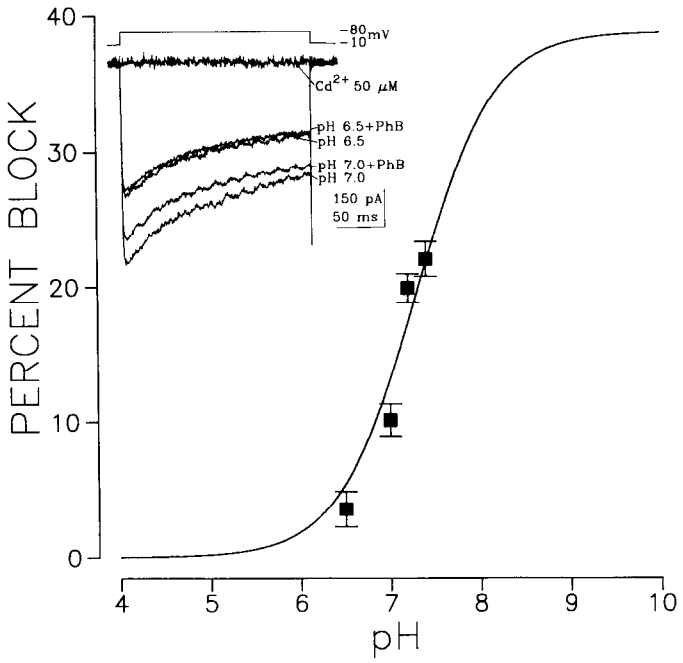

Figure 4. Percentage block of I_{Ca} upon superfusion with solutions of 10 μM PHB at various pH values. Each data point represents the mean ± SEM of three or four cells. The *smooth curve* is the appropriately scaled titration curve for PHB (pK_a, 7.29) where the ordinate value is the percentage dissociated (anionic).

bonyl group of PHB is shown by the solid line. This curve is given by the function $B_{max}/(1 + 10^{7.29 - pH})$, where the scale factor B_{max} (=39%) was estimated by a nonlinear least-squares fit to the experimental data. It is apparent that the reduction in the blocking effect of PHB closely matches the titration curve for the acidic group on PHB, indicating that the anionic form of the molecule is the active species. In addition to diminishing the block produced by PHB, low pH also produced a moderate suppression of I_{Ca} (Fig. 4, inset).

(−)-PB block of I_{Ca} *is voltage dependent*

Although (−)-PB reduced I_{Ca} over a wide range of membrane potentials (Fig. 1*B*), the degree of block increased as the step potential became more positive. If the (−)-PB blocking site is within the electrical field of the membrane and if the active form of the molecule is the anion (as is the case for PHB), positive membrane potentials should tend to enhance binding. [The pK_a of PB is 8.0 (Narahashi et al., 1971), so approximately 20% of the molecules are in the anionic form at physiological pH.] The increase in block at positive membrane potentials was analyzed according to the scheme of Woodhull (1973) in which the binding affinity is assumed to vary exponentially with the membrane potential and the blocking drug does not interact with other ions. In this model, the ratio of current in the absence and presence of (−)-PB, I_0/I_{PB}, can be related to the transmembrane voltage, V, according to the relationship

$$I_0/I_{PB} = 1 + \{[PCP]/K_D(0)\}e^{-z\delta FV/RT}, \quad (3)$$

where $K_D(0)$ represents the dissociation constant of the (−)-PB–acceptor site complex at 0 transmembrane potential, δ is the fractional voltage drop experienced at the acceptor site (measured from the outside), z is the charge of (−)-PB (=−1), and

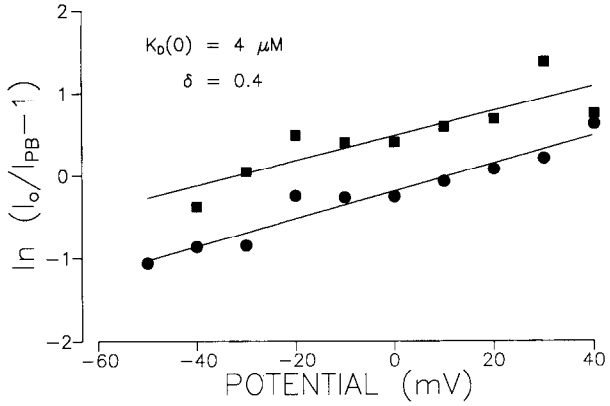

Figure 5. (−)-PB depresses I_{Ca} in a voltage-dependent manner with increasing block as the membrane potential is brought to more positive levels. Data are from two separate experiments with 1 (●) and 10 (■) μM (−)-PB. The *straight lines* are the linear least-square fits to the data according to Equation 3; the means of the derived parameters are as shown.

F, R, and T have their usual meanings. $K_D(0)$ and δ were determined from a plot of ln $(I_0/I_{(-)\text{-PB}} - 1)$ against V, as shown in Figure 5 for 1 μM and 10 μM (−)-PB. The mean value of $K_D(0)$ was 4 μM. Correcting this value to −10 mV using the equation $K_D(V) = K_D(0)e^{z\delta FV/RT}$ (see Woodhull, 1973), we obtain a $K_D(-10)$ of 3.4 μM. This independent measure of the K_D for (−)-PB block of I_{Ca} is almost identical to the K_D value of 3.5 μM determined by titration at −10 mV (Fig. 3). The mean value of δ was 0.4, which indicates that the (−)-PB blocking site senses approximately 40% of the transmembrane electric field measured from the outside.

(−)-PB and PHB do not alter the activation of I_{Ca}

We investigated the time course and voltage dependence for activation of I_{Ca} using the extrapolated tail current amplitudes (at −80 mV). The tail current amplitudes provide an estimate of the instantaneous conductance at the end of the depolarizing step. Figure 6A_1 illustrates a family of Ca^{2+} channel currents and their tail currents evoked by depolarizing steps of increasing duration from 0.5 to 6 msec in 0.5 msec increments. The Ca^{2+} channel currents and the corresponding tail currents were reduced in amplitude by 10 μM (−)-PB (Fig. 6A_2). However, as shown in Figure 6A_3, the rate of activation of the Ca^{2+} conductance (τ = 1.02 msec), as determined from the extrapolated tail current amplitudes, was not altered by the drug. Similar results were obtained in three additional cells with (−)-PB. PHB also failed to alter the rate of activation of the Ca^{2+} conductance (n = 4; not shown).

We next investigated the effect of (−)-PB on the voltage dependence for activation of the Ca^{2+} conductance. Figure 6B_1 illustrates the tail currents following 10 msec duration steps to −10 and +20 mV. In this cell, superfusion with 10 μM (−)-PB results in a marked reduction in the tail current amplitudes at both potentials (Fig. 6B_2). Despite the large suppression of the current, as illustrated in Figure 6B_3, which plots the fraction of the maximum extrapolated tail current amplitude versus the step potential, the current–voltage relationship for the residual current was similar to that of the control current. Similar results were obtained in three additional cells. The smooth curve in Figure 6B_3 was drawn by fitting the data points to the Boltzmann function $[1 + e^{(V_{1/2} - V)/A}]^{-1}$ with $V_{1/2}$ = −12.5 mV and A = 16

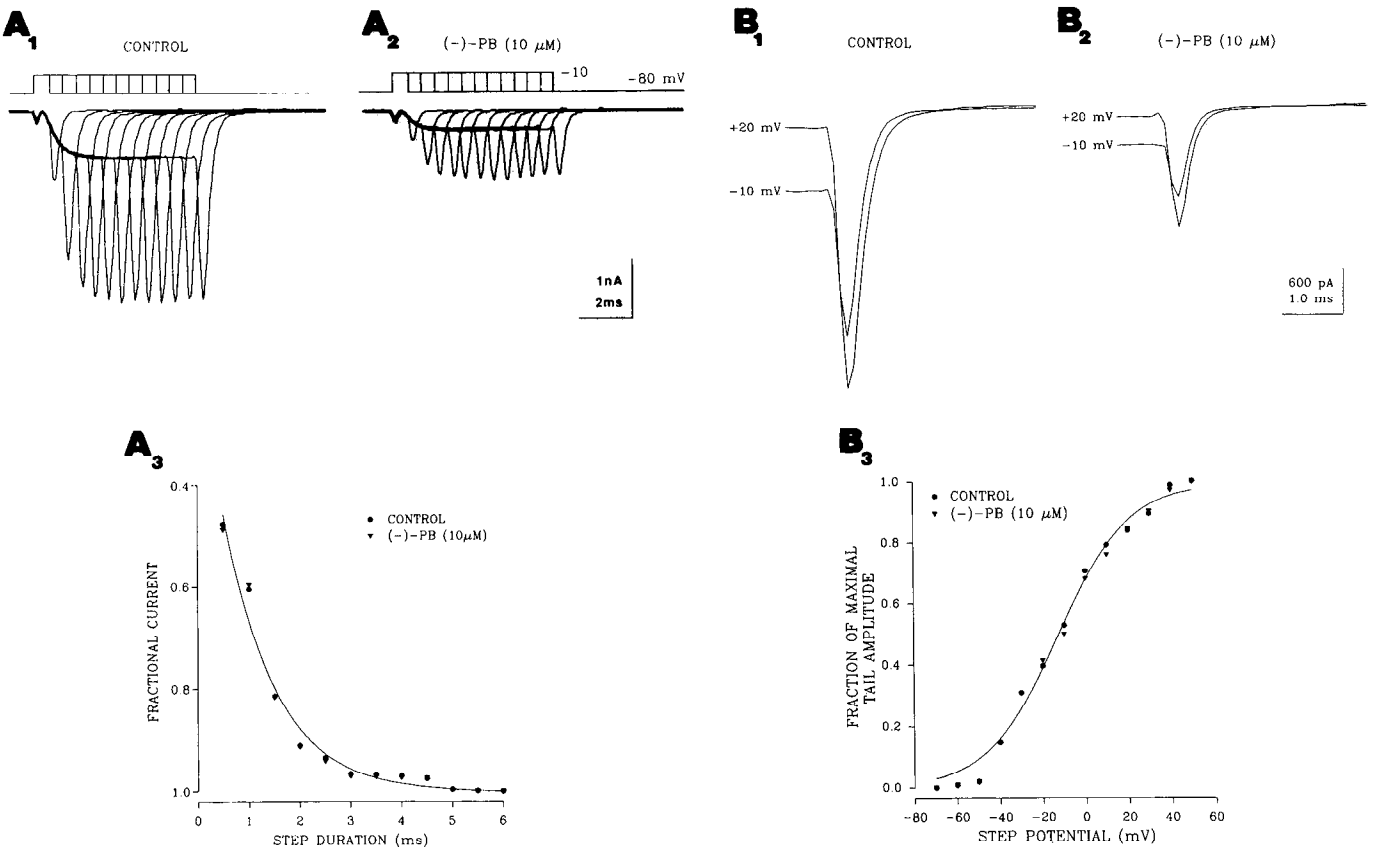

Figure 6. *A*, (−)-PB does not alter the time course of I_{Ca} activation. Tail currents were elicited by depolarizing voltage steps (from −80 to −10 mV) of various durations (0.5–6 msec, 0.5 msec increments) in the absence (A_1) and presence (A_2) of 10 μM (−)-PB. The interval between successive steps was 1 sec. A_3, Extrapolated tail current amplitudes (at −80 mV) normalized to the maximum tail current amplitude (6 msec step); the *solid line* is the best single-exponential fit to the control and (−)-PB data; time constant, 1.02 msec. *B*, (−)-PB does not alter the voltage dependence of I_{Ca} activation: tail currents following 10-msec-duration voltage steps from −80 mV to −10 and +20 mV in the absence (B_1) and presence (B_2) of 10 μM (−)-PB. B_3, Tail current amplitudes at −80 mV normalized to the maximal value [either control or (−)-PB] following activation of current by test pulses to various potentials. The *smooth curve* was drawn by fitting the data points to a Boltzmann function (see Results) with half-maximal voltage ($V_{1/2}$) of −12.5 mV and slope factor (A) of 16 mV. The points between −70 and −40 mV are likely to be underestimates of the true values because of the difficulty of measuring the small tail currents at these potentials. The interval between successive steps in each family was 6 sec.

mV. PHB also failed to alter the voltage dependence of activation of I_{Ca} (n = 3; data not shown).

(−)-PB speeds I_{Ca} *inactivation*

During prolonged voltage steps, I_{Ca} gradually inactivated but did not reach a plateau even with steps as long as 1 sec in duration. The inward current showed an initial, rapid decline followed by a more gradual decay (see, e.g., Fig. 7*A*). A consistent observation with all of the barbiturates tested was a greater block of the late current than the peak current as illustrated in Figure 7*A*. For example, with 1 μM (−)-PB, there was 32 ± 4% block of the peak current and a 60 ± 9% block of the current at 1 sec after the onset of the step ($p < 0.05$, paired t test; n = 5 cells). The inactivation during 1 sec steps was adequately fit by the sum of the two exponential functions with voltage-dependent time constants (τ_{fast} and τ_{slow}). The augmented block of the late current was due to a speeding of both τ_{fast} and τ_{slow}, but the effect on τ_{slow} was much larger. For example, for the cell illustrated in Figure 7*A*, τ_{fast} and τ_{slow} were 69 msec and 573 msec, respectively, while in the presence of 1 μM (−)-PB the corresponding values were 60 msec and 288 msec. The concentration dependence of the effect of (−)-PB on τ_{fast} and τ_{slow} is summarized in Table 2. Increasing concentrations of (−)-PB did not significantly affect τ_{fast} but speeded τ_{slow}. The rate of decay of I_{Ca} was dependent upon membrane potential, with a monotonic slowing of both τ_{fast} and τ_{slow} as the step potential was made more positive. CHEB (300 μM) caused a similar effect on the two time constants of inactivation: τ_{fast} and τ_{slow} were, respectively, 49 and 377 msec under control conditions and 46 and 267 msec in the presence of the drug (means of data from two cells).

To investigate inactivation throughout the range of membrane potentials at which Ca^{2+} channels are conducting, we used a two-pulse voltage-clamp protocol in which inactivation was allowed to proceed during a 1 sec voltage step and the current passing capacity of the noninactivated channels was assessed at the end of the step with a 100 msec postpulse to −10 mV (Fig. 7*A*). Using this protocol, we are able to estimate the degree of inactivation at potentials where little current is flowing through the open channels because of a small driving force. In Figure 7*B*, the prepulse peak inward current (○, ●) and test pulse peak inward current (□, ■) are plotted as a function of prepulse potential. The extent of inactivation as assessed by the postpulse current did not show a monotonic increase with increasing prepulse potential (Fig. 7*B*, □), as is typical of many voltage-dependent channels. Instead, the inactivation curve had an inverted U-shape, with inactivation greatest at −10 mV, a potential near the maximum of the current (−20 mV). The inactivation curve during 1 μM (−)-PB (■) was similar in shape to the control

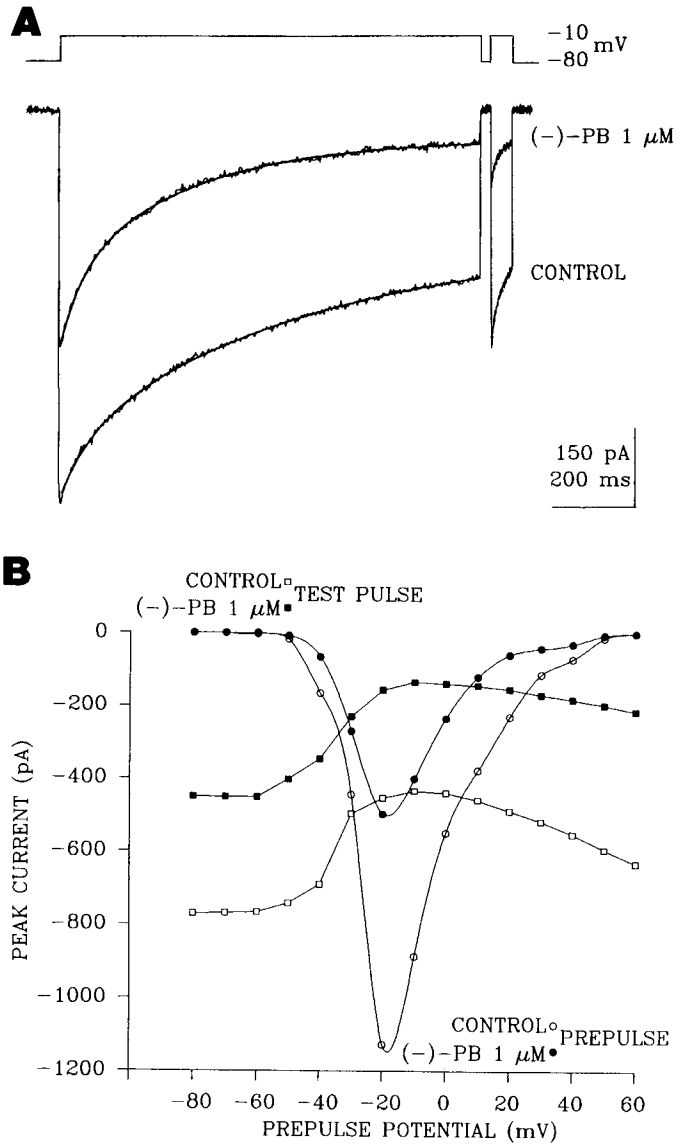

Figure 7. Voltage dependence of inactivation of I_{Ca} during 1 sec depolarizing steps to various step potentials from a holding potential of −80 mV. *A*, A double pulse protocol was used to determine the level of inactivation at the end of a 1 sec step. The postpulse step is always from −80 to −10 mV with a 22 msec interval between the prepulse and postpulse. The prepulse inactivated according to a biexponential time course (best fit superimposed on the raw trace) with τ_{fast} = 69 msec and τ_{slow} = 573 msec. In the presence of 1 μM (−)-PB, corresponding values are τ_{fast} = 60 msec and τ_{slow} = 288 msec. *B*, Prepulse peak current (○, ●) plotted and test pulse peak current (□, ■) plotted against prepulse potential. The data points are connected by cubic splines.

curve, but showed a greater absolute extent of inactivation at all prepulse potentials and also a relatively greater degree of inactivation at potentials positive to −10 mV. The inverted U-shape inactivation curve and the specific effect of (−)-PB portrayed in Figure 7*B* were observed in all cells examined (n = 3). Although an inverted U-shape inactivation curve is typical of current-dependent inactivation, we have previously provided strong evidence that inactivation under the conditions used in this study (Ba^{2+} as charge carrier) is largely independent of current (ffrench-Mullen and Rogawski, 1992; see also Jones and Marks, 1989; Kay, 1991). Consequently, the results imply an effect of (−)-PB on channel gating and not on the disposition of intracellular cations.

Table 2. Effect of (−)-PB on the time constants of Ca^{2+} channel current inactivation

		(−)-PB		
Time constant	Control	0.1 μM	1.0 μM	10 μM
τ_{fast} (msec)	41 ± 2	44 ± 2	39 ± 4	43 ± 4
τ_{slow} (msec)	437 ± 14	403 ± 24	269 ± 22*	260 ± 20*

Ca^{2+} channel current was activated with 1 sec steps from −80 to −10 mV. The evoked current was fit to a biexponential function using a nonlinear curve fitting routine. Each value represents the mean of data from four cells.

* Significantly different from control, $p < 0.05$ (paired t test).

Since (−)-PB block of I_{Ca} is greater at depolarized potentials, a possible mechanism to account for the speeding of the apparent rate of I_{Ca} inactivation is that there is a slow transition in the degree of block from the level at the holding potential (−80 mV) to the greater level at the step potential (−10 mV). An apparent speeding of the slow phase of I_{Ca} inactivation would be manifest if the rates of transition occurred on a time scale comparable to that of slow inactivation. To investigate this possibility, we determined the fractional block of I_{Ca} at each of the 1000 points acquired during 1 sec voltage steps in the presence of 1, 10, and 20 μM (−)-PB. As illustrated in Figure 8*C*, the time constants of the fits to the fractional block values increase with increasing (−)-PB concentration. Assuming a first-order bimolecular binding reaction between the drug and the channel, the rate of approach to equilibrium $k_{app} = k_1[(-)\text{-PB}] + k_{-1}$, where k_1 and k_{-1} are the forward and reverse binding rates. We calculated the k_{app} values as the reciprocal of the time constants of the fits to the fractional block data and plotted them against concentration. For the cell shown in Figure 8*A*, the concentration-dependent increase in rate was consistent with the proposed mechanism and, from the plot shown in Figure 8*C*, we estimated $k_1 = 1.1 \times 10^5\ M^{-1}sec^{-1}$ and $k_{-1} = 3.2 \times 10^6\ sec^{-1}$ (at −10 mV). However, we were unable to carry out additional experiments as our supply of (−)-PB became exhausted.

Barbiturates enhance GABA-activated Cl^- current

The effects of (−)- and (+)-PB and PHB were investigated on GABA-activated Cl^- current evoked with 10–200 msec applications of GABA. The inward current activated by GABA at −50 mV was completely blocked by 10 μM picrotoxin (n = 3; Fig. 9*B*). As illustrated in Figure 9, *A* and *B*, (−)-PB and PHB enhanced the amplitude and duration of the GABA response in a concentration-dependent fashion. The concentration–response relationships for these effects are presented in Figure 10, and the EC_{50} and P_{max} values are summarized in Table 1. The P_{max} value for PHB was 600%, compared to a P_{max} value of 1366% for (−)-PB, indicating that PHB has a partial agonist-like effect. Figure 10 also illustrates that 1 mM (±)-PB produces a similar potentiation of GABA responses as does (−)-PB, a result that is expected since the (−)-enantiomer component of the racemate would by itself produce a maximal (plateau) response.

Figure 9, *C* and *D*, demonstrates the voltage-independent action of (−)-PB on GABA-activated Cl^- current. The GABA current was enhanced throughout the range of voltages tested (−50 to +30 mV), without affecting its reversal potential (−3.5 mV) or modifying its voltage dependence. Similar results were obtained in two additional cells; the mean reversal potential was −2.9 ± 0.35 mV (n = 3) and this was taken to be the equilibrium

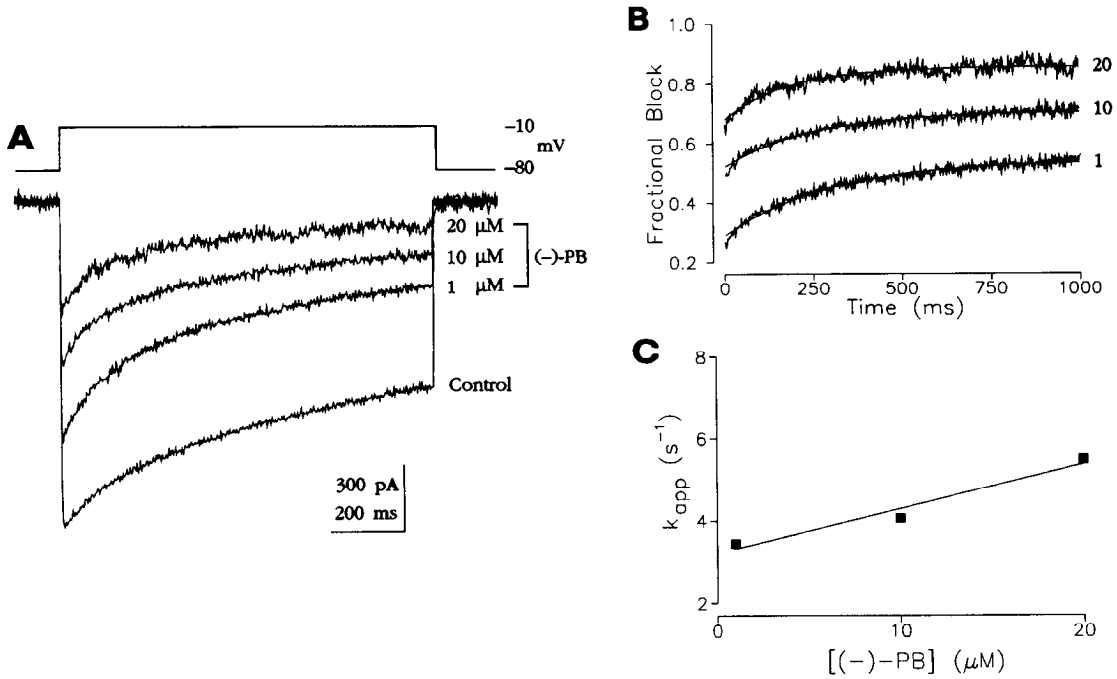

Figure 8. Concentration dependence of the apparent speeding in I_{Ca} inactivation rate produced by (−)-PB. *A*, Current records illustrating the block of I_{Ca} by 1, 10, and 20 μM (−)-PB. *B*, Fractional block values computed with respect to the control current at each point in the current traces shown in *A*. The *thin curves* illustrate the best single exponential fits to the data points. *C*, Apparent rate constant values (k_{app}) estimated as the reciprocals of the time constants of the exponential fits to the fractional block values shown in *B*. The *straight line* is the least-squares best fit to the data.

potential for Cl^-. At concentrations greater than 100 μM, (−)-PB and PHB directly activated Cl^- current even in the absence of GABA, as did (+)-PB at 1 mM (not shown).

Discussion

The principal observation in this study is that the sedative–anesthetic barbiturate PB produces a potent, stereoselective blockade of a voltage-activated Ca^{2+} channel current in CA1 hippocampal neurons. This effect occurs at concentrations similar to those that potentiate GABA responses. In contrast, the anticonvulsant barbiturate PHB was substantially weaker as a blocker of Ca^{2+} channel current than as a potentiator of GABA responses and the maximal GABA response potentiation obtained was only 44% of that obtained with PB. Therefore, the CNS depression produced by the active *S*(−)-enantiomer of PB may reflect a powerful action of the drug on both Ca^{2+} channels and GABA receptors, whereas the anticonvulsant effect of PHB at therapeutic concentrations may be due to a more modest enhancement of GABA responses and submaximal block of Ca^{2+} channels.

The effect of PB on Ca^{2+} channel current and GABA receptor responses occurred in a stereoselective fashion, with the *S*(−)-enantiomer being more potent than the *R*(+)-enantiomer. This stereoselectivity corresponds with that exhibited by the isomers as CNS depressants *in vivo* (Wadell and Baggett, 1973; Richter and Holtman, 1982). In contrast, it has recently been reported that the (+)- and (−)-isomers of PB are equipotent at depressing voltage-dependent Na^+ channels (Frenkel et al., 1990) and that they have opposite stereoselectivity for binding to nicotinic cholinergic receptors (Roth et al., 1989), implying that effects on these channels do not contribute in a major way to the sedative action of the drug. In contrast, (−)-PB was more potent than (+)-PB in enhancing a slow outward current in *Aplysia* giant neurons (Huguenard and Wilson, 1985); however, the significance of this action with regard to the depressant effects of the drug in the mammalian CNS is uncertain.

PHB was substantially less potent than (−)-PB both in suppressing Ca^{2+} channel current and in potentiating GABA responses. However, in contrast to the situation with (−)-PB, where the two effects occurred at similar concentrations, PHB was weaker as a Ca^{2+} channel blocker than as a GABA enhancer. In patients receiving therapeutic doses of PHB, the free serum concentrations of the drug are typically 25–100 μM (Prichard and Ransom, 1989). At these concentrations, our results predict substantial enhancement of GABA responses (i.e., the therapeutic range is on the upper part of the rising phase of the concentration–response curve). However, the maximal GABA potentiation produced by PHB was less than that of PB and this could contribute to the relatively weaker CNS depressant activity of PHB.

Although there is variation among individuals, free serum concentrations of PHB >100 μM frequently produce sedation (Prichard and Ransom, 1989). At these concentrations, enhancement of GABA responses would be only slightly greater than at therapeutic levels, but there would be substantially larger blockade of Ca^{2+} current, suggesting that effects on Ca^{2+} current may be important to the sedative side effects of PHB at supratherapeutic blood levels. At concentrations greater than 100 μM, we note that both (−)-PB and PHB activate a Cl^- current response by themselves, even in the absence of GABA; this direct agonist action, which has been observed previously in CNS neurons (Barker and Ransom, 1978; Nicoll and Wojtowicz, 1980) and also in *Xenopus* oocytes expressing cloned $GABA_A$ receptor subunits (Levitan et al., 1988), could be an additional

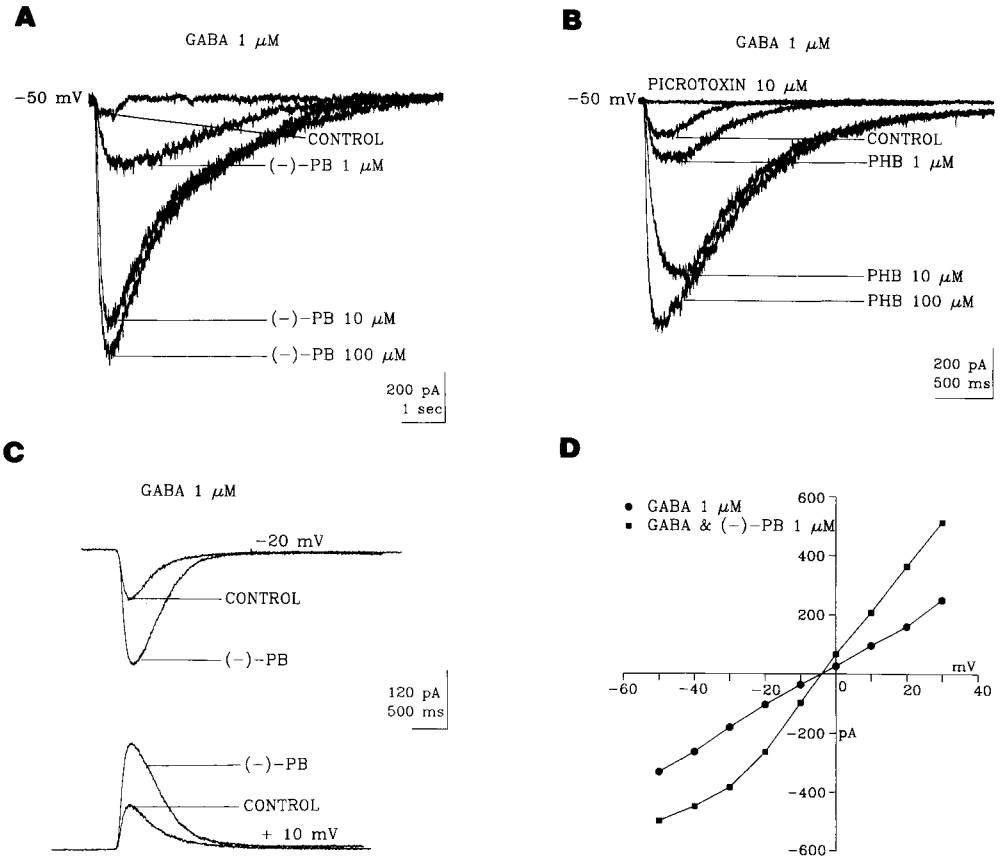

Figure 9. Barbiturate enhancement of the GABA-activated Cl^- current. *A*, Concentration-dependent effect of (−)-PB on Cl^- current evoked with 50-msec-duration applications of 1 μM GABA at a holding potential of −50 mV. *B*, Effect of PHB in another cell. The GABA-activated current was completely blocked by 10 μM picrotoxin. Note the difference in the size of the control response compared with that in *A*. *C*, Representative GABA currents at −20 and +10 mV in the absence (control) and presence of 1 μM (−)-PB. *D*, Current–voltage relationship for the cell illustrated in *C*.

factor contributing to the CNS depressant activity of the barbiturates at high doses (Macdonald and Barker, 1978; Schulz and Macdonald, 1981).

Prompted by the observation that barbiturates suppress presynaptic release of neurotransmitters and reduce Ca^{2+} entry into synaptosomes (see introductory remarks), several groups have investigated the action of barbiturates on voltage-dependent Ca^{2+} currents in invertebrate (Ikemoto et al., 1986; Nishi and Oyama, 1983) and vertebrate (Werz and Macdonald, 1985; Gross and Macdonald, 1988) neurons. These investigators have generally observed that PB suppresses certain Ca^{2+} current components by enhancing steady-state inactivation and markedly accelerating the rate of inactivation. However, these studies in invertebrate and peripheral vertebrate neurons typically required PB concentrations > 100 μM to obtain substantial block of the current (IC_{50} ~ 250 μM). Similarly, the IC_{50} for blockade of Ca^{2+} current in *Xenopus* oocytes injected with total human brain mRNA was ~250 μM (Gundersen et al., 1988). In contrast, the Ca^{2+} current activated by depolarization of acutely isolated CA1 hippocampal neurons from a holding potential of −80 mV was blocked by 70-fold lower concentrations of PB. At least some of potency differences may relate to differences in the method of drug application. In the present series of experiments we utilized a fast perfusion system that delivers drug solutions with little dilution, whereas in previous studies drugs were often applied by diffusion or pressure ejection from micropipettes in a manner that could result in substantial mixing with the bath solution. However, it is unlikely that technical factors alone can completely account for the apparent potency differences. In mouse sensory neurons, Gross and Macdonald (1988) have proposed that there is differential sensitivity of various Ca^{2+} channel types to barbiturates that selectively block N- and L- but not T-type Ca^{2+} currents. Similarly, the Ca^{2+} channel current in CA1 hippocampal neurons appears particularly sensitive to block by barbiturates. The total Ca^{2+} current activated by depolarization from −80 mV in these cells may consist of several components (Regan et al., 1991; ffrench-Mullen and Plata-Salamán, 1992; Mintz et al., 1992). The concentration–response data presented in Figure 3 indicate that the barbiturates block

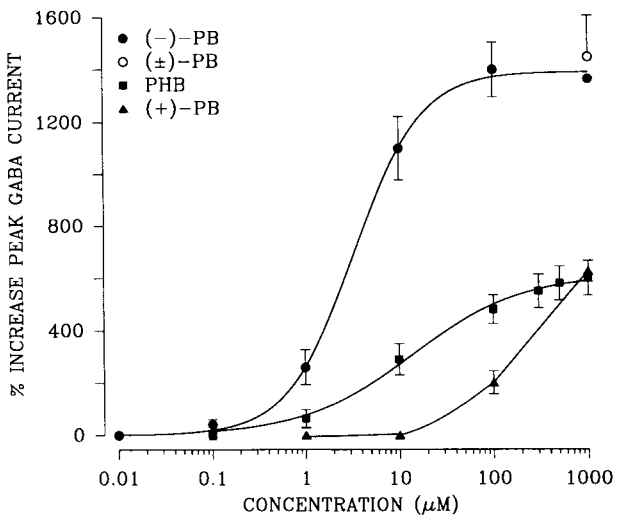

Figure 10. Concentration–response curves for the potentiation of GABA current. The EC_{50} and P_{max} values are given in Table 1. Each point represents the mean ± SEM of three or four cells.

all of the components (100% block at 1 mM). Moreover, our data taken together indicate that the sensitivity of the various components may be roughly similar. However, this preliminary conclusion will need to be examined further using selective antagonists to separate the components.

As previously reported for the Ca^{2+} channels in sensory neurons and human brain mRNA-injected oocytes (Gross and Macdonald, 1988; Gundersen et al., 1988), neither (−)-PB nor PHB had any effect on the shape of the current–voltage relationship of the Ca^{2+} channel current in CA1 hippocampal neurons. Moreover, the drug failed to alter the voltage dependence of channel activation and did not affect the channel activation kinetics. In addition, it is noteworthy that there was no use dependence to the block with either (−)-PB or PHB, in contrast to our previous results with phencyclidine in the same preparation (ffrench-Mullen and Rogawski, 1992). [The lack of use dependence here differs from the situation in snail neurons; see Nishi and Oyama (1983).] (−)-PB's block of the Ca^{2+} current occurred in a voltage-dependent fashion, with the degree of block increasing as the membrane was brought to more positive potentials. The voltage dependence of the (−)-PB block at pH 7.40 indicates that the (−)-PB acceptor site senses about 40% of the transmembrane electric field, and implies that the charged form of the molecule is the active species. This conclusion is similar to that obtained by Blaustein (1968) for PB block of Na^+ and K^+ channels in lobster axons, but opposite to that of other investigators (Krupp et al., 1969; Narahashi et al., 1971; Nishi and Oyama, 1983). The discrepancy may, in part, reflect the fact that at alkaline pH, the uncharged barbiturate molecule would be able to penetrate tissue more effectively. Thus, even if the charged form is the active one, high pH could favor block under certain circumstances because higher drug concentrations would be achieved at the blocking site (but see Krupp et al., 1969). In any case, block of I_{Ca} by PHB matched the titration curve for the acid group, providing additional evidence that the charged forms of the barbiturate molecules are responsible for channel block in the present situation. We note, however, that this conclusion is only valid if the shift in pH does not modify the intrinsic sensitivity of the Ca^{2+} channel to block by PHB. Potentiation of GABA-activated Cl^- current by (−)-PB was insensitive to voltage, indicating that the (−)-PB acceptor site is outside the transmembrane electric field or, alternatively, that the uncharged form of the molecule is the active species.

There are several mechanisms that could account for the acceleration in the rate of inactivation produced by the barbiturates. Gross and Macdonald (1988) have speculated that PB may enhance inactivation of the N-type Ca^{2+} current in mouse sensory neurons by increasing the efficacy of Ca^{2+}-dependent inactivation. This is unlikely in the present circumstance since we strongly chelated internal Ca^{2+} and used Ba^{2+} as the charge carrier. [Ba^{2+} does not support current-dependent Ca^{2+} channel inactivation under the present conditions; see ffrench-Mullen and Rogawski (1992).] A similar conclusion was obtained by Nishi and Oyama (1983), who studied the effect of PB on the inactivation of Ca^{2+} current in *Helix* neurons internally perfused with high concentrations of EGTA. These investigators proposed that PB accelerates inactivation by an open channel blocking mechanism because it appeared to act in an use-dependent fashion when applied during trains. We did not observe any use dependence to the (−)-PB block. Thus, our data indicate that (−)-PB can bind and block closed channels, and an open channel blocking mechanism is unlikely to account for the block in the present study. However, the affinity of the drug for closed channels at −80 mV differs from that at −10 mV because repulsive electric field effects on the anionic (−)-PB molecule are diminished at the depolarized potential. The concentration-dependent increase in slow inactivation rate (Table 2) and the more detailed, but preliminary analysis presented in Figure 8 suggest that the apparent speeding of I_{Ca} inactivation produced by (−)-PB may to a large extent reflect the slow transition from the level of block at −80 mV to that at −10 mV. Thus, the barbiturates appear to modify the gating of the Ca^{2+} channels allosterically to reduce the total number of channels available for activation and to enhance steady-state inactivation (Fig. 7); there may not be a meaningful effect on the rate of inactivation per se. However, a more specific definition of the step(s) in the gating reaction affected by barbiturates will require a more detailed understanding of the gating of the Ca^{2+} channels.

The convulsant barbiturate CHEB blocked Ca^{2+} channel current in a similar manner as the other barbiturates, although it was weaker than either (−)-PB or PHB. Convulsant barbiturates including CHEB have previously been reported to potentiate GABA receptor responses and shorten Ca^{2+}-dependent action potentials (presumably by inhibiting Ca^{2+} channels) in a similar fashion as sedative and anticonvulsant barbiturates (Skerritt and Macdonald, 1984; Holland et al., 1990); in addition, they may have other cellular actions that account for their convulsant activity (Downes and Franz, 1971; Nicholson et al., 1988a,b). Our demonstration that CHEB is an effective blocker of Ca^{2+} channel current is consistent with these previous reports. However, the effect on Ca^{2+} channels does not provide insight into the convulsant activity of the drug.

References

Andrews PR, Jones GP, Pulton DB (1982) Convulsant, anticonvulsant and anaesthetic barbiturates. *In vivo* activities of oxo- and thiobarbiturates related to pentobarbitone. Eur J Pharmacol 79:61–65.

Barker JL, Ransom BR (1978) Pentobarbitone pharmacology of mammalian central neurones grown in tissue culture. J Physiol (Lond) 280: 355–372.

Bean BP (1989) Classes of calcium channels in vertebrate cells. Annu Rev Physiol 51:367–384.

Blaustein MP (1968) Barbiturates block sodium and potassium conductance increases in voltage-clamped lobster axons. J Gen Physiol 51:293–307.

Blaustein MP, Ector AC (1975) Barbiturate inhibition of calcium uptake by depolarized nerve terminals *in vitro*. Mol Pharmacol 11:369–378.

Brooks CM, Eccles JC (1947) A study of the effect of anesthesia on the monosynaptic pathway of the spinal chord. J Neurophysiol 10: 340–360.

Byerly L, Yazejian B (1986) Intracellular factors for the maintenance of calcium currents in perfused neurones from the snail, *Lymnaea stagnalis*. J Physiol (Lond) 370:631–650.

Downes H, Franz DN (1971) Effects of a convulsant barbiturate on dorsal root ganglion cells and dorsal root discharges. J Pharmacol Exp Ther 179:660–670.

Eckert R, Chad JE (1984) Inactivation of Ca channels. Prog Biophys Mol Biol 44:215–267.

ffrench-Mullen JMH, Plata-Salamán CR (1992) Interleukin-1β inhibition of calcium channel currents in isolated hippocampal CA1 neurons: pharmacology and mode of action. Soc Neurosci Abstr 18:433.

ffrench-Mullen JMH, Rogawski MA (1992) Phencyclidine block of calcium current in isolated guinea-pig hippocampal neurones. J Physiol (Lond) 456:85–105.

Forscher P, Oxford GS (1985) Modulation of calcium channels by norepinephrine in internally dialyzed avian sensory neurons. J Gen Physiol 85:743–763.

Frenkel CE, Duch DS, Urban BW (1990) Molecular actions of pen-

tobarbital isomers on sodium channels from human brain cortex. Anesthesiology 72:640–649.
Gross RA, Macdonald RL (1988) Differential actions of pentobarbitone on calcium current components of mouse sensory neurons in culture. J Physiol (Lond) 405:187–203.
Gundersen CB, Umbach JA, Swartz BE (1988) Barbiturates depress currents through human brain calcium channels studied in *Xenopus* oocytes. J Pharmacol Exp Ther 247:824–829.
Holland KD, Canney DJ, Rothman SM, Ferrendelli JA, Covey DF (1990) Physiological modulation of the GABA receptor by convulsant and anticonvulsant barbiturates in cultured rat hippocampal neurons. Brain Res 516:147–150.
Huguenard JR, Wilson WA (1985) Barbiturate-induced alterations in the kinetic parameters of slow outward current in *Aplysia* giant neurons. J Pharmacol Exp Ther 234:821–829.
Ikemoto Y, Mitsuiye T, Ishizuka S (1986) Reduction of the voltage-dependent calcium current in *Aplysia* neurons by pentobarbital. Cell Mol Biol 6:293–305.
Jones SW, Marks TN (1989) Calcium current in bullfrog sympathetic neurons. I. Inactivation. J Gen Physiol 94:169–182.
Kay AR (1991) Inactivation kinctics of calcium current of acutely dissociated CA1 pyramidal cells of the mature guinea-pig hippocampus. J Physiol (Lond) 437:27–48.
Kay AR, Wong RKS (1986) Isolation of neurons suitable for patch-clamping from adult mammalian central nervous system. J Neurosci Methods 16:227–238.
Krupp P, Bianchi CP, Suarez-Kurtz G (1969) On the local anaesthetic effect of barbiturates. J Pharm Pharmacol 21:763–768.
Leslie SW, Friedman MB, Wilcox RE, Elrod SV (1980) Acute and chronic effects of barbiturates on depolarization-induced calcium influx into rat synaptosomes. Brain Res 185:409–417.
Levitan ES, Blair LAC, Dionne VE, Barnard EA (1988) Biophysical and pharmacological properties of cloned $GABA_A$ receptor subunits expressed in *Xenopus* oocytes. Neuron 1:773–781.
Macdonald RL, Barker JL (1979) Anticonvulsant and anesthetic barbiturates: different postsynaptic actions in cultured mammalian neurons. Neurology 29:432–447.
Macdonald RL, Rogers CJ, Twyman RE (1989) Barbiturate regulation of kinetic properties of the $GABA_A$ receptor channel of mouse spinal neurones in culture. J Physiol (Lond) 417:483–500.
Mathers DA, Barker JL (1980) (−)-Pentobarbital opens ion channels of long duration in cultured mouse spinal neurons. Science 209:507–509.
Miller RJ (1990) Receptor-mediated regulation of calcium channels and neurotransmitter release. FASEB J 4:3291–3299.
Mintz IA, Adams ME, Bean BP (1992) P-type calcium channels in rat central and peripheral neurons. Neuron 9:85–95.
Morgan KG, Bryant SH (1977) Pentobarbital: presynaptic effect in the squid giant synapse. Experientia 33:487–488.
Narahashi T, Frazier DT, Deguchi T, Cleaves CA, Ernau MC (1971) The active form of pentobarbital in squid giant axons. J Pharmacol Exp Ther 177:25–33.
Nicholson GM, Spence I, Johnston GAR (1988a) Differing actions of convulsant and nonconvulsant barbiturates: an electrophysiological study in the isolated spinal cord of the rat. Neuropharmacology 27: 459–465.
Nicholson GM, Spence I, Johnston GAR (1988b) Depolarizing actions of convulsant barbiturates on isolated rat dorsal root ganglion cells. Neurosci Lett 93:330–335.
Nicoll RA, Wojtowicz JM (1980) The effects of pentobarbital and related compounds on frog motoneurons. Brain Res 191:225–237.
Nicoll RA, Eccles JC, Oshima T, Rubia F (1975) Prolongation of hippocampal inhibitory postsynaptic potentials by barbiturates. Nature 258:625–627.
Nishi K, Oyama Y (1983) Accelerating effects of pentobarbitone on the inactivation process of the calcium current in *Helix* neurones. Br J Pharmacol 79:645–654.
Olsen RW (1988) Barbiturates. Int Anesthesiol Clin 26:254–261.
Parker I, Gundersen CB, Miledi R (1986) Actions of pentobarbital on rat brain expressed in *Xenopus* oocytes. J Neurosci 6:2290–2297.
Prichard JW, Ransom BR (1989) Phenobarbital. Mechanisms of action. In: Antiepileptic drugs, 3d ed (Levy R, Mattson R, Meldrum B, Penry JK, Dreifuss FE, eds), pp 267–282. New York: Raven.
Rall TW (1990) Hypnotics and sedatives: ethanol. In: Goodman and Gilman's the pharmacological basis of therapeutics, 8th ed (Gilman AG, Rall RT, Nies AS, Taylor P, eds), pp 345–382. New York: Pergamon.
Regan LJ, Sah DWY, Bean BP (1991) Ca^{2+} channels in rat central and peripheral neurons: high-threshold current resistant to dihydropyridine blockers and omega-conotoxin. Neuron 6:269–280.
Richards CD (1972) On the mechanism of barbiturate anaesthesia. J Physiol (Lond) 227:749–767.
Richter JA, Holtman JR Jr (1982) Barbiturates: their *in vivo* effects and potential biochemical mechanisms. Prog Neurobiol 18:275–319.
Rogawski MA, Porter RJ (1990) Antiepileptic drugs: pharmacological mechanisms and clinical efficacy with consideration of promising developmental stage compounds. Pharmacol Rev 42:223–286.
Roth SH, Forman SA, Braswell LM, Miller KW (1989) Actions of pentobarbital enantiomers on nicotinic cholinergic receptors. Mol Pharmacol 36:874–880.
Schulz DW, Macdonald RL (1981) Barbiturate enhancement of GABA-mediated inhibition and activation of a chloride ion conductance: correlation with anticonvulsant and anesthetic actions. Brain Res 209: 177–188.
Skerritt JH, Macdonald RL (1984) Multiple actions of convulsant barbiturates on mouse neurons in cell culture. J Pharmacol Exp Ther 230:82–88.
Stanley EF (1991) Single-calcium channels on a cholinergic presynaptic nerve terminal. Neuron 7:585–591.
Thompson SM, Wong RKS (1991) Development of calcium current subtypes in isolated rat hippocampal pyramidal cells. J Physiol (Lond) 439:671–689.
Vida JA, Gerry EH (1977) Cyclic ureides. In: Anticonvulsants (Vida JA, ed), pp 151–291. New York: Raven.
Waddell WJ, Baggett B (1973) Anesthetic and lethal activity in mice of the stereoisomers of 5-ethyl-5-(1-methybutyl) barbituric acid (pentobarbital). Arch Int Pharmacodyn Ther 205:40–44.
Weakly JN (1969) Effect of barbiturates on "quantal" synaptic transmission in spinal motor neurones. J Physiol (Lond) 204:63–77.
Werz MA, Macdonald RL (1985) Barbiturates decrease voltage-dependent calcium conductance of mouse neurons in dissociated cell culture. Mol Pharmacol 28:269–277.
Woodhull AM (1973) Ionic blockage of sodium channels in nerve. J Gen Physiol 61:687–708.